

# SOME REMARKS ON FINITE ELEMENTS WITH AN ELLIPTIC HOLE

Reinhard Piltner

Department of Mathematical Sciences,  
Georgia Southern University, Statesboro, GA 30460-8093, U.S.A.  
e-mail: rpiltner@georgiasouthern.edu

**Abstract.** *Some issues regarding the implementation of finite elements with elliptic holes are discussed. Although the treatment of rigid body modes appears to be different for Trefftz functions satisfying boundary conditions on circular holes from those functions ensuring the satisfaction of boundary conditions on elliptic holes, the programming can be done similarly. For the investigation of the numerical performance of hole elements using a larger number of Trefftz functions, a 24-node hole element is compared to 8-node and 16-node elements. Details of the implementation issues are given.*

**Key words:** Hybrid-Trefftz finite elements, complex functions, stress concentration, elasticity

## 1 Introduction

Building on the basic idea of Erich Trefftz [35] many papers have been written on how to utilize a set of linearly independent trial functions, which a priori satisfy the differential equation under consideration, for obtaining approximate solutions [1-40]. The papers include the use of the Trefftz method for boundary elements and finite elements. Since the Trefftz functions satisfy the governing differential equations, domain integrals vanish, and it becomes possible to compute finite element stiffness matrices via boundary integrals evaluated along the finite element boundary. The author presented in reference [21] 8-node and 16-node elements with circular and elliptic holes. In a recent publication [2], the authors questioned the reliability of the hole elements if a larger number of Trefftz terms is used. In this paper the details of the implementation not discussed before are given. In the numerical example section the results for a 24-node hole element are compared to results obtained with 8-node and 16-node hole elements. The conclusions in this study are different from the statements presented in reference [2].

## 2 Governing differential equations and complex solution representation

For plane strain and plane stress we can give the solution for the homogeneous Navier-equations

$$\begin{aligned}\mu\Delta u + (\lambda + \mu) \frac{\partial e}{\partial x} &= 0 \\ \mu\Delta v + (\lambda + \mu) \frac{\partial e}{\partial y} &= 0\end{aligned}\tag{1}$$

in complex form as

$$\begin{aligned}2\mu u &= \operatorname{Re}[\kappa\Phi(z) - z\overline{\Phi'(z)} - \overline{\Psi(z)}] \\ 2\mu v &= \operatorname{Im}[\kappa\Phi(z) - z\overline{\Phi'(z)} - \overline{\Psi(z)}]\end{aligned}\tag{2}$$

where

$$\begin{aligned}e &= u_x + v_y \\ \mu &= \frac{E}{2(1+\nu)} \\ \lambda &= \begin{cases} \frac{E\nu}{1+\nu^2} & \text{for plane stress} \\ \frac{E\nu}{(1+\nu)(1-2\nu)} & \text{for plane strain} \end{cases}\end{aligned}\tag{3}$$

and

$$\kappa = \begin{cases} (3 - \nu)/(1 + \nu) & \text{for plane stress} \\ (3 - 4\nu) & \text{for plane strain} \end{cases}\tag{4}$$

have been used.

For given displacements  $\bar{u}$  and  $\bar{v}$  the boundary conditions can be written as

$$\kappa\Phi(z) - z\overline{\Phi'(z)} - \overline{\Psi(z)} = 2\mu(\bar{u} + i\bar{v}) \quad \text{on } \Gamma_u\tag{5}$$

whereas for given tractions  $\bar{T}_x$  and  $\bar{T}_y$  the complex form for the boundary conditions is given by

$$\Phi(z) + z\overline{\Phi'(z)} + \overline{\Psi(z)} = i \int (\bar{T}_x + i\bar{T}_y) ds \quad \text{on } \Gamma_T .\tag{6}$$

When using a conformal mapping  $z = f(\zeta)$  involving the complex variable  $\zeta = \xi + i\eta$ , one has to distinguish the derivatives

$$\Phi'(z) = \frac{d\Phi(z)}{dz} \quad (7)$$

and

$$\dot{\Phi}(\zeta) = \frac{d\Phi(\zeta)}{d\zeta} . \quad (8)$$

The function  $\Phi$  is assumed in the transformed domain (i.e.  $\Phi = \Phi(\zeta)$ ). Therefore we need the following derivatives

$$\Phi' = \frac{\dot{\Phi}(\zeta)}{\dot{f}(\zeta)} \quad (9)$$

and

$$\Phi'' = \frac{\ddot{\Phi}(\zeta)}{\dot{f}^2(\zeta)} - \dot{\Phi}(\zeta) \frac{\ddot{f}(\zeta)}{\dot{f}^3(\zeta)} . \quad (10)$$

for the computation of the stresses

$$\sigma_{xx} = Re[2\Phi'(z) - \bar{z}\Phi''(z) - \Psi'(z)] \quad (11)$$

$$\sigma_{yy} = Re[2\Phi'(z) + \bar{z}\Phi''(z) + \Psi'(z)] \quad (12)$$

$$\tau_{xy} = Im[\bar{z}\Phi''(z) + \Psi'(z)] \quad (13)$$

### 3 Functions for finite elements with elliptic holes

For the construction of Trefftz functions for a finite element with an elliptic hole, the finite element domain is mapped to a new domain (Figure 1). The mapping illustrated in Figure 1 allows us to consider boundary conditions on a unit circle instead of more difficult boundary conditions on the boundary of the elliptic hole. The conformal mapping

$$z = f(\zeta) = c\left(\zeta + \frac{m}{\zeta}\right) \quad (14)$$

involves the semiaxes  $a$  and  $b$  of the ellipse:

$$c = \frac{a+b}{2} \quad (15)$$

$$m = \frac{a-b}{a+b} . \quad (16)$$

On the unit circle we have the following feature for the complex variable  $\zeta = \xi + i\eta$ :

$$\bar{\zeta}^j = \zeta^{-j} \quad \text{on } |\zeta| = 1 . \quad (17)$$

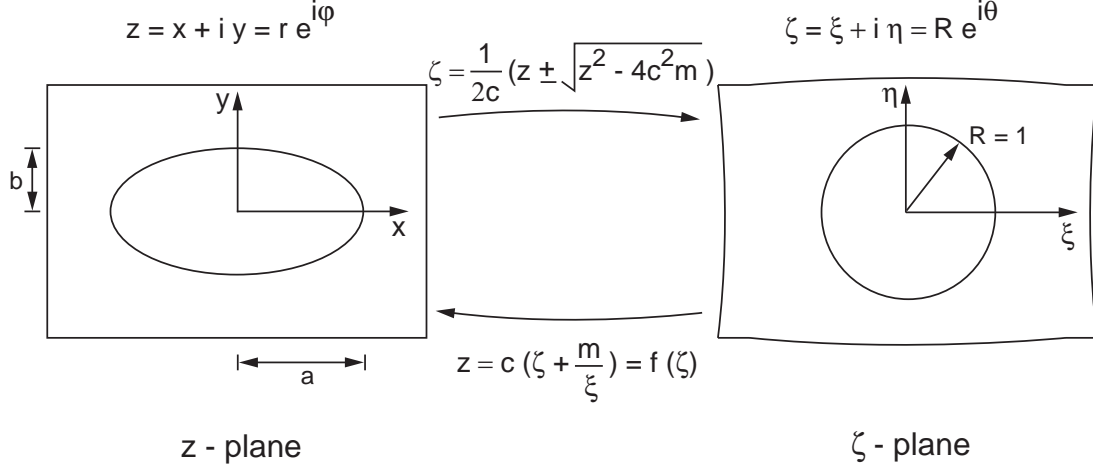


Figure 1: Mapping of a finite element with an elliptic hole.

The traction-free boundary condition on the unit circle can be written as

$$\Psi(\zeta) = -\overline{\Phi(\zeta)} - \overline{f(\zeta)} \frac{\dot{\Phi}(\zeta)}{\dot{f}(\zeta)} \quad \text{on } |\zeta| = 1 . \quad (18)$$

Because the derivative of  $f$  of the mapping function is not a constant for a general ellipse, the following substitution turns out to be convenient:

$$\Psi(\zeta) = \frac{\dot{\chi}(\zeta)}{\dot{f}(\zeta)} . \quad (19)$$

The boundary condition becomes

$$\dot{\chi}(\zeta) = -\dot{f}(\zeta) \overline{\Phi(\zeta)} - \overline{f(\zeta)} \dot{\Phi}(\zeta) \quad \text{on } |\zeta| = 1 . \quad (20)$$

With a chosen  $\Phi$  of the form

$$\Phi(\zeta) = \sum_{j=-N}^M a_j \zeta^j \quad (21)$$

and utilizing the feature (17) on the unit circle, the expression for  $\dot{\chi}$  is obtained as

$$\dot{\chi}(\zeta) = -c \sum_{j=-N}^M \bar{a}_j \zeta^{-j} + cm \sum_{j=-N}^M \bar{a}_j \zeta^{-j-2} - c \sum_{j=-N}^M j a_j \zeta^{j-2} - cm \sum_{j=-N}^M j a_j \zeta^j . \quad (22)$$

For a general ellipse the function  $\Psi$  is obtained from the substitution (19).

For the first example element shown in Figure 2, the summation limits are chosen as  $N = 4$  and  $M = 4$ , and between two adjacent nodes linear boundary displacements are assumed. For the second element and the third element in Figure 2, the limits are chosen as  $N = 8$  and  $M = 8$ , and boundary displacements are chosen as piecewise quadratic functions.

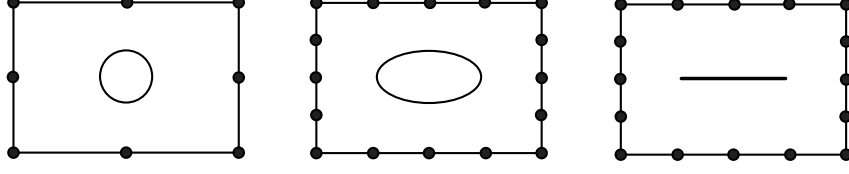


Figure 2: Finite elements with a circular/elliptic hole and with an internal crack.

### 3.1 Functions for a circular hole

For the special case of a circular hole, the parameter  $m$  takes the value  $m = 0$  and the function  $\Psi$  can be written as

$$\Psi(\zeta) = - \sum_{j=-N}^M j a_j \zeta^{j-2} - \sum_{j=-N}^M \bar{a}_j \zeta^{-j} . \quad (23)$$

The pair of functions  $\Phi$  and  $\Psi$  from equations (21) and (23) guarantee the satisfaction of both the equilibrium equations and the boundary conditions on the hole boundary.

### 3.2 Complex functions for non-homogenous boundary conditions

For the case of constant pressure  $p$  on the hole we obtain

$$i \int (\bar{T}_x + i\bar{T}_y) ds = -pz = -pc\left(\zeta + \frac{m}{\zeta}\right) \quad (24)$$

In order to satisfy the stress boundary condition

$$\Phi(\zeta) + f(\zeta) \frac{\bar{\Phi}(\zeta)}{\bar{f}(\zeta)} + \bar{\Psi}(\zeta) = i \int (\bar{T}_x + i\bar{T}_y) ds \quad (25)$$

we can choose the following complex functions:

$$\Phi = 0 , \Psi = -pc\left(\frac{1}{\zeta} + m\zeta\right) \quad (26)$$

For a constant shear load  $q$  on the elliptic boundary we can choose

$$\Phi = 0 , \Psi = -iqc\left(\frac{1}{\zeta} + m\zeta\right) \quad (27)$$

## 4 Rigid body terms

The displacement functions (2) include the three rigid body terms. However it is not easy to identify these terms because the complex functions had been assumed in the  $\zeta$ -plane instead of the  $z$ -plane. In order to identify the rigid body terms we can look at the stress terms and search for entries with zeros. However, for the case of a rigid body rotation, a rigid body term and a deformation term already present in the series are superposed. The terms responsible for the two rigid body translation are

$$\Phi = a_0 \tag{28}$$

and

$$\Psi = \frac{-c\bar{a}_0 + cma_0\zeta^{-2}}{c[1 - m\zeta^{-2}]} = -\bar{a}_0 \tag{29}$$

With  $a_0 = \alpha_0 + i\beta_0$  we get the rigid body displacements

$$u_{trans} = \frac{1}{2\mu}(\kappa + 1)\alpha_0 \tag{30}$$

$$v_{trans} = \frac{1}{2\mu}(\kappa + 1)\beta_0 \tag{31}$$

Equation (29) shows that the rigid body translation terms should be programmed differently from the other terms in order to avoid the dependence on  $\zeta$  which will cancel out. For the mixed finite element the terms with  $\alpha_0$  and  $\beta_0$  will be omitted. A rigid body rotation can be obtained from  $\Phi(z) = i\beta_1 z$  or in the  $\zeta$ -plane from the complex functions

$$\Phi(\zeta) = ic\left[\zeta + \frac{m}{\zeta}\right]\beta_1 \text{ and } \Psi = 0\beta_1 \tag{32}$$

However, we do not recognize these terms in the series for  $\Phi$  and  $\Psi$ . The relevant terms are

$$\Phi = i\beta_1\zeta + i\beta_{-1}\zeta^{-1} \tag{33}$$

$$\Psi = \frac{-imc[\zeta + \zeta^{-3}]}{c[1 - m\zeta^{-2}]} \beta_1 + \frac{ic[\zeta + \zeta^{-3}]}{c[1 - m\zeta^{-2}]} \beta_{-1} \tag{34}$$

Note that the terms in (34) are not linearly independent, and that there are non-vanishing stresses associated with  $\beta_1$ -terms. In order to make the rigid body rotation visible we add and immediately subtract  $im\beta_1\zeta^{-1}$  in (33):

$$\Phi = i\beta_1\zeta + i\beta_{-1}\zeta^{-1} + im\beta_1\zeta^{-1} - im\beta_1\zeta^{-1} \quad (35)$$

This leads to the rotation term plus two linearly dependent terms:

$$\Phi = i [\zeta + m\zeta^{-1}] \beta_1 + i\beta_{-1}\zeta^{-1} - im\beta_1\zeta^{-1} \quad (36)$$

Instead of superposing the rigid body rotation term with a term that is already included in the series with the  $\beta_{-1}$ -term, we could use the following simplified pair of complex functions with coefficients  $\beta_1$  and  $\beta_{-1}$ :

$$\begin{aligned} \Phi &= i [\zeta + m\zeta^{-1}] \beta_1 + i\beta_{-1}\zeta^{-1} \\ \Psi &= 0\beta_1 + \frac{ic[\zeta + \zeta^{-3}]}{c[1 - m\zeta^{-2}]} \beta_{-1} \end{aligned} \quad (37)$$

The simplification effects only the terms involving  $\beta_1$ . For the mixed finite element application the terms with  $\beta_1$  will be removed.

## 5 Variational formulation and stiffness matrix

Utilizing functions which satisfy the governing differential equations, the variational formulation reduces to

$$\delta\Pi = - \int_S \delta\mathbf{T}^T(\mathbf{u} - \tilde{\mathbf{u}})dS + \int_S \delta\mathbf{u}^T(\mathbf{T} - \bar{\mathbf{T}})dS \quad (38)$$

where  $\mathbf{T} = \mathbf{nEDu}$ ,  $\mathbf{u}$  are the Trefftz displacement functions obtained from the complex solution representation, and  $\tilde{\mathbf{u}}$  are the assumed boundary displacements along the element boundary. The assumed boundary displacements involve the nodal displacements  $\mathbf{q}$ , and the Trefftz functions collected in  $\mathbf{u}$  involve parameters which are eliminated at the element level. With the Trefftz functions

$$\mathbf{u} = \begin{bmatrix} \mathbf{U} \\ \mathbf{V} \end{bmatrix} \boldsymbol{\beta} \quad (39)$$

$$\mathbf{T} = \begin{bmatrix} \mathbf{T}_x \\ \mathbf{T}_y \end{bmatrix} \boldsymbol{\beta} \quad (40)$$

and the boundary displacements

$$\tilde{\mathbf{u}} = \begin{bmatrix} \tilde{u} \\ \tilde{v} \end{bmatrix} = \begin{bmatrix} \tilde{\mathbf{U}} & \mathbf{0} \\ \mathbf{0} & \tilde{\mathbf{V}} \end{bmatrix} \mathbf{q} \quad (41)$$

the element stiffness matrix can be computed as

$$\mathbf{k} = \mathbf{L}^T \mathbf{H}^{-1} \mathbf{L} \quad (42)$$

where

$$\mathbf{H} = \int_S \frac{1}{2} [\mathbf{U}^T \mathbf{T}_x + \mathbf{T}_x^T \mathbf{U} + \mathbf{V}^T \mathbf{T}_y + \mathbf{T}_y^T \mathbf{V}] dS \quad (43)$$

and

$$\mathbf{L} = \left[ \int_S \mathbf{T}_x^T \tilde{\mathbf{U}} dS \quad \int_S \mathbf{T}_y^T \tilde{\mathbf{V}} dS \right] \quad (44)$$

Since the Trefftz functions satisfy the boundary conditions on the boundary of the hole the numerical integration has to be done only along the outer boundary of the hole element. The stiffness matrix for the hybrid Trefftz element with a hole has three zero eigenvalues.

## 6 Discussion about the number of stress terms needed

In a hybrid method the relationship between the number of stress terms  $n_\beta$  and the number of nodal displacements  $n_q$  is given by

$$n_\beta \geq n_q - r \quad (45)$$

For a plane strain/stress problem we have  $r = 3$  rigid body modes. From the complex functions,  $2(N + M + 1)$  Trefftz functions are generated. After removing the rigid body terms we have  $(2N + 2M - 1)$  Trefftz functions for the elements with holes.  $N$  and  $M$  have to be chosen such that relationship (45) will be satisfied. It is known for a long time that choosing too many stress terms is counter productive and will yield an element which is too stiff. It is desirable to have  $n_\beta = n_q - r$ . However, this is not always possible in the design of hybrid-Trefftz elements. In Table 1 the parameters for the chosen 8-node, 16-node and 24-node elements are listed.

	Boundary displacements	N (N=M)	$n_\beta = 2N + 2M - 1$	$n_q$
8-node element	Piecewise linear	4	15	16
16-node element	Piecewise quadratic	8	31	32
24-node element	Piecewise linear	12	47	48

Table 1: Parameters for elements with elliptic hole.

## 7 Utilizing Symmetry for rectangular elements

The outer boundary of the hole element can have a quadrilateral or polygonal shape. For the special case of a rectangular outer boundary one can utilize the features of odd and

even functions and get all information for the computation of  $\mathbf{H}$  and  $\mathbf{L}$  from integrating along one half or even along one quarter of the element boundary. For rectangular elements the matrix  $\mathbf{H}$  has the following structure:

$$\mathbf{H} = \begin{bmatrix} \mathbf{H}_{11} & \mathbf{0} \\ \mathbf{0} & \mathbf{H}_{22} \end{bmatrix} \quad (46)$$

## 8 Integration along the boundary

For piecewise linear boundary displacements each integration interval between two neighboring nodal points is divided into 10 subintervals. For each subinterval a Gauss quadrature formula with three points is chosen. Using a boundary coordinate  $s$  with  $s=0$  at node  $i$  and  $s=1$  at node  $j$  we compute the following quantities:

$$s_{ij} = \sqrt{(x_j - x_i)^2 + (y_j - y_i)^2} \quad (47)$$

$$n_x = \frac{y_j - y_i}{s_{ij}}, \quad n_y = -\frac{x_j - x_i}{s_{ij}} \quad (48)$$

$$x = \left(1 - \frac{s}{s_{ij}}\right)x_i + \frac{s}{s_{ij}}x_j \quad (49)$$

$$y = \left(1 - \frac{s}{s_{ij}}\right)y_i + \frac{s}{s_{ij}}y_j \quad (50)$$

After computing  $x$ ,  $y$  for a Gauss point, the  $\xi$ ,  $\eta$  coordinates are computed via the conformal mapping function.

## 9 Numerical examples

Examples for which exact solutions are available have been chosen to demonstrate the accuracy of the 8-node, 16-node, and 24-node elliptic hole elements (Figure 3).

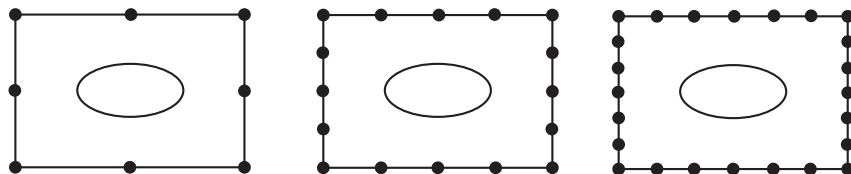


Figure 3: 8-node, 16-node, and 24-node elements with an elliptic hole.

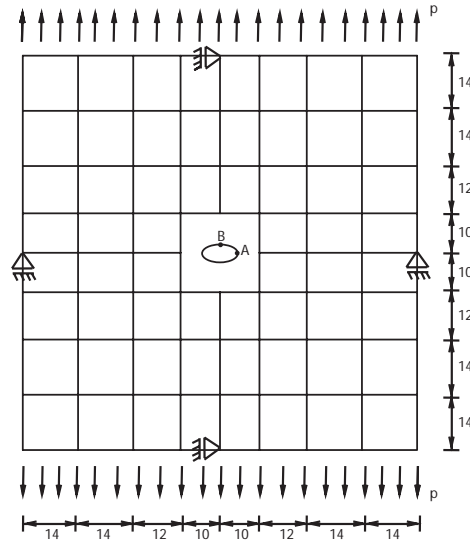


Figure 4: Finite element mesh with 60 displacement elements and one 8-node hole element.

### 9.1 Example 1: Plate with elliptic hole under tension

A plate with an elliptic hole has been analyzed using displacement elements and a hybrid Trefftz element with a hole (Figures 4 and 5). Figure 5 shows the mesh used for the 24-node hole element. For the examples, plane stress has been assumed, and the parameters have been chosen as  $E = 1$ ,  $\nu = 0.3$ , and  $p = 1$ . The numerical results for the stress concentration values are summarized in Tables 2, 3, 4, and 5.

a/b	1	2	6	20
exact	3.0	5.0	13.0	41.0
8-node element with piecewise linear disp.	2.993	4.991	12.96	40.92
Error	0.2%	0.2%	0.3%	0.2%

Table 2: Hoop stress at point A inside the 8-node element for different ratios a/b, a=2.

a/b	1	2	6	20
exact	-1.0	-1.0	-1.0	-1.0
8-node element with piecewise linear disp.	-0.995	-0.996	-0.995	-0.998
Error	0.5%	0.4%	0.5%	0.2%

Table 3: Stress  $\sigma_{xx}/p$  at point B inside the 8-node element for different ratios a/b, a=2.

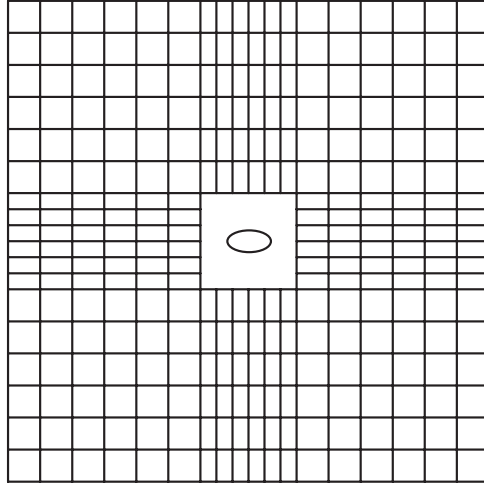


Figure 5: Finite element mesh with 288 displacement elements and one 24-node hole element.

a/b	1	2	6	20
exact	3.0	5.0	13.0	41.0
24-node element with piecewise linear disp.	3.005	5.006	13.01	41.04
Error	0.2%	0.1%	0.1%	0.1%

Table 4: Hoop stress at point A inside the 24-node element for different ratios a/b, a=2.

a/b	1	2	6	20
exact	-1.0	-1.0	-1.0	-1.0
24-node element with piecewise linear disp.	-1.004	-1.002	-1.001	-1.001
Error	0.4%	0.2%	0.1%	0.1%

Table 5: Stress  $\sigma_{xx}/p$  at point B inside the 24-node element for different ratios a/b, a=2.

## 9.2 Example 2: Plate with internal crack under tension

The meshes shown in Figures 4 and 5 are used for analyzing a plate with an internal crack. The semi axis of the elliptic hole is chosen as  $b=0$ . The 24-node element gave the best results for the stress intensity factors (Table 6). However the 8-node and 16-node element already provide very good results. The 24-node element gave for the second stress intensity factor  $K_{II} = 0.9 * 10^{-15}$  instead of the exact value  $K_{II} = 0$ .

	8-node element	16-node element	24-node element	Exact ( $K_I = \sqrt{a}$ )
$K_I$	1.412	1.4164	1.4154	1.4142
error	0.16%	0.15%	0.08%	

Table 6: Stress intensity factor  $K_I$  for plate with internal crack of length  $2a=4$  using different elliptic hole elements ( $a=2$ ,  $b=0$ ).

## 10 Concluding remarks

Details of the implementation issues of elements with an elliptic hole have been discussed. Elements with 15, 31, and 47 Trefftz functions have been studied. For problems with an internal crack the 24-node element with 47 Trefftz terms gave the best numerical results for the stress intensity factors. This study did not show a loss of accuracy with an increase in the number of Trefftz terms as suggested in reference [2]. All elements considered here have a good balance between the number of Trefftz terms and the total number of element degrees of freedom. The stress concentration errors in this study were much smaller than those reported in reference [2].

## References

- [1] J.P.B.M. Almeida, O.J.B.A. Pereira: "A Set of Hybrid Equilibrium Finite Element Models for the Analysis of Three-Dimensional Solids". International Journal for Numerical Methods in Engineering, **39**, 2789-2802, (1996).
- [2] M. Dhanasekar, Jianjun Han and Qinghua Qin: "A hybrid -Trefftz element containing an elliptic hole". Finite Elements in Analysis and Design, **42**, 1314 - 1323, (2006).
- [3] N.A. Dumont: "The hybrid boundary element method: An alliance between mechanical consistency and simplicity". Appl. Mech. Rev., **42(11)**, S54 -63, (1989).
- [4] J.A. Teixeira de Freitas and Z.Y. Ji: "Hybrid-Trefftz equilibrium model for crack problems". Int. J. Numer. Meth. Eng., **39**, 569 - 584, (1996).

- [5] J. A. Teixeira de Freitas: "*Formulation of elastostatic hybrid-Trefftz stress elements*". Computer Methods in Applied Mechanics and Engineering, **153**, 127-151, (1998).
- [6] I. Herrera: "*Trefftz Method: A General Theory*". Numerical Methods for Partial Differential Equations, **16(6)**, 561 - 580, (2000).
- [7] J. Jirousek: "*Basis for development of large finite elements locally satisfying all field equations*", Comp. Meth. Appl. Mech. Engrg., **14**, 65 - 92, (1978).
- [8] J. Jirousek: "*Hybrid-Trefftz plate bending elements with p-method capabilities*", Int. J. Numer. Meth. Eng., **24**, 1367 - 1393, (1987).
- [9] J. Jirousek, A. Venkatesh: "*Hybrid Trefftz plane elasticity elements with p-method capabilities*", Int. J. Numer. Meth. Eng., **35**, 1443 - 1472, (1992).
- [10] J. Jirousek, A. Wroblewski, Q.H. Qin, X.Q. He: "*A family of quadrilateral hybrid Trefftz p-elements for thick plate analysis*", Comp. Meth. Appl. Mech. Engrg., **127**, 315 - 344, (1995).
- [11] J. Jirousek, A.P. Zielinski and A. Wroblewski: "*T-element analysis of plates on unilateral elastic Winkler-type foundation*", Comp. Ass. Meth. Engrg. Sci., **8**, 343 - 358, (2001).
- [12] E. Kita and N. Kamiya: "*Trefftz method: an overview*", Advances in Engineering Software, **24**, 3 - 12, (1995).
- [13] V. Kompis, F. Konkol, M. Vasko: "*Trefftz-polynomial reciprocity based FE formulations*", Computer Assist. Mech. Eng. Sci, **8**, 385 - 395, (2001).
- [14] V.M.A. Leitão: "*On a multi-region indirect Trefftz formulation for potential problems*", Engineering Analysis with Boundary Elements, **12**, 77-96, (1997).
- [15] V.M.A. Leitão: "*Application of multi-region Trefftz-collocation to fracture mechanics*", Engineering Analysis with Boundary Elements, **22**, 251-256, (1998).
- [16] E.A.W. Maunder, J.P.B.M. Almeida: "*Hybrid-equilibrium elements with control of spurious kinematic modes*". Computer Assisted Mechanics and Engineering Sciences **4**, 587-605, (1997).
- [17] E.A.W. Maunder, J.P.B.M. Almeida, A.C.A. Ramsay: "*A General Formulation of Equilibrium Macro-Elements with Control of Spurious Kinematic Modes*". International Journal for Numerical Methods in Engineering **39**, 3175-3194, (1996).
- [18] S. Moorthy and S. Ghosh: "*Model for analysis of arbitrary composite and porous microstructures with Voronoi cell finite elements*", Int. J. Numer. Meth. Eng., **39**, 2363 - 2398, (1996).
- [19] N.I. Muskhelishvili: "*Some Basic Problems of the Mathematical Theory of Elasticity*". Noordhoff, Groningen, The Netherlands, 1953.

- [20] J. Petrolito: "*Hybrid-Trefftz quadrilateral elements for thick plate analysis*". *Comp. Meth. Appl. Mech. Engrg.*, **78(3)**, 331-351,(1990).
- [21] R. Piltner, "*Special finite elements with holes and internal cracks*", *Int. J. Numer. Meth. Eng.*, **21**, 1471 - 1485, (1985).
- [22] R. Piltner: "*The application of a complex 3-dimensional elasticity solution representation for the analysis of a thick rectangular plate*", *Acta Mechanica* **75**, 77 - 91, (1988).
- [23] R. Piltner: "*The derivation of a thick and thin plate formulation without ad hoc assumptions*", *Journal of Elasticity*, **29**, 133 - 173, (1992).
- [24] R. Piltner: "*Three-dimensional stress and displacement representations for plate problems*", *Mechanics Research Communications*, **18 (1)**, 41 - 49, (1991).
- [25] R. Piltner: "*A quadrilateral hybrid Trefftz plate bending element for the inclusion of warping based on a three-dimensional plate formulation*", *Int. J. Numer. Meth. Eng.* **33**, 387 - 408, (1992).
- [26] R. Piltner: "*On the representation of three-dimensional elasticity solutions with the aid of complex valued functions*", *Journal of Elasticity*, **22**, 45 - 55, (1989).
- [27] R. Piltner and R.L. Taylor: "*A quadrilateral mixed finite element with two enhanced strain modes*", *Int. J. Numer. Meth. Eng.* **38**, 1783 - 1808, (1995).
- [28] Q.-H. Qin: *The Trefftz finite and boundary element method*. WIT Press, Southampton, (2000).
- [29] S. Reutsky, B. Tirozzi: "*Spectral Method for Elliptic Equations of General Type*". *Comp. Ass. Mech. and Eng. Sci.*, **8(4)**, 629 - 644, (2001).
- [30] G. Ruoff: "*Die praktische Berechnung der Kopplungsmatrizen bei der Kombination der Trefftzschen Methode und der Methode der finiten Elemente*". In *Finite Elemente in der Statik*, Verlag Ernst & Sohn, Berlin, 1973, pp. 242 - 259.
- [31] E. Stein: "*Die Kombination des modifizierten Trefftzschen Verfahrens mit der Methode der finiten Elemente*". In *Finite Elemente in der Statik*, Verlag Ernst & Sohn, Berlin, 1973, pp. 172 - 185.
- [32] E. Stein: "*An appreciation of Erich Trefftz*". *Comp. Ass. Mech. and Eng. Sci.*, **4**, 301 - 304, (1997).
- [33] B. Szabo and I. Babuska: *Finite Element Analysis*. John Wiley & Sons, New York, (1991).
- [34] P. Tong, T.H.H. Pian and S. Lasry: "A hybrid element approach to crack problems in plane elasticity", *Int. J. Numer. Meth. Eng.*, **7**, 297 - 308, (1973).
- [35] E. Trefftz: "Ein Gegenstück zum Ritzschen Verfahren", 2. Int. Kongr. für Techn. Mech., Zürich, 1926, pp. 131 - 137.

- [36] J. Zhang and N. Katsube: "A hybrid finite element method for heterogeneous materials with randomly dispersed rigid inclusions", *Int. J. Numer. Meth. Eng.*, **38**, 1635 - 1653, (1995).
- [37] A.P. Zielinski, O.C. Zienkiewicz: "*Generalized finite element analysis with T-complete boundary solution functions*". *Int. J. Numer. Meth. Eng.*, **21**, 509 - 528, (1985).
- [38] A.P. Zielinski: "*On trial functions applied in the generalized Trefftz method*". *Advances in Engineering Software*, **25**, 147 - 155, (1995).
- [39] O.C. Zienkiewicz, D.W. Kelly and P. Bettess: "*The coupling of finite element and boundary solution procedures*". *Int. J. Numer. Meth. Eng.*, **11**, 355 - 376, (1977).
- [40] O.C. Zienkiewicz and R.L. Taylor: *The Finite Element Method. Vol. 1/2*. McGraw Hill, New York, 1989/1991.